### RESEARCH ARTICLE

# Intensification and poleward shift of subtropical western boundary currents in a warming climate

**Hu Yang[1], Gerrit Lohmann[1,2], Wei Wei[1], Mihai Dima[1,3], Monica Ionita[1], and Jiping Liu[4]**

[1]Climate Sciences, Alfred Wegener Institute, Helmholtz Centre for Polar and Marine Research, Bremerhaven, Germany, [2]Department of Environmental Physics, University of Bremen, Bremen, Germany, [3]Faculty of Physics, University of Bucharest, Bucharest, Romania, [4]Department of Atmospheric and Environmental Sciences, University at Albany, State University of New York, Albany, New York, USA

**Abstract** A significant increase in sea surface temperature (SST) is observed over the midlatitude western boundary currents (WBCs) during the past century. However, the mechanism for this phenomenon remains poorly understood due to limited observations. In the present paper, several coupled parameters (i.e., sea surface temperature (SST), ocean surface heat fluxes, ocean water velocity, ocean surface winds and sea level pressure (SLP)) are analyzed to identify the dynamic changes of the WBCs. Three types of independent data sets are used, including reanalysis products, satellite-blended observations. and climate model outputs from the fifth phase of the Climate Model Intercomparison Project (CMIP5). Based on these broad ranges of data, we find that the WBCs (except the Gulf Stream) are intensifying and shifting toward the poles as long-term effects of global warming. An intensification and poleward shift of near-surface ocean winds, attributed to positive annular mode-like trends, are proposed to be the forcing of such dynamic changes. In contrast to the other WBCs, the Gulf Stream is expected to be weaker under global warming, which is most likely related to a weakening of the Atlantic Meridional Overturning Circulation (AMOC). However, we also notice that the natural variations of WBCs might conceal the long-term effect of global warming in the available observational data sets, especially over the Northern Hemisphere. Therefore, long-term observations or proxy data are necessary to further evaluate the dynamics of the WBCs.

## 1. Introduction

The subtropical western boundary currents (WBCs), including the Kuroshio Current, the Gulf Stream, the Brazil Current, the East Australian Current, and the Agulhas Current, are the western branches of the subtropical gyres. They are characterized by fast ocean velocities, sharp sea surface temperature (SST) fronts, and intensive ocean heat loss. The strength and routes of WBCs have a broad impact on the weather and climate over the adjacent mainland. For instance, WBCs regions favor the formation of severe storms [*Kelly et al.*, 1996; *Inatsu et al.*, 2002; *Taguchi et al.*, 2009; *Cronin et al.*, 2010], while the poleward ocean heat transport by the WBCs contributes to the global heat balance [*Colling*, 2001].

In recent years, there has been an increasing interest in the variability of WBCs under global warming. *Deser et al.* [1999] suggested that there has been a decadal intensification of Kuroshio Current during the 1970–1980 period due to a decadal variation in wind stress curl, whereas *Sato et al.* [2006] and *Sakamoto et al.* [2005] projected a stronger Kuroshio Current in response to global warming according to a high-resolution coupled atmosphere-ocean climate model. *Curry and McCartney* [2001] found that the transport of the Gulf Stream has intensified after the 1960s, which is attributed to a stronger North Atlantic Oscillation. In agreement with *Curry and McCartney* [2001], an increase in the storm frequency has also been recorded in extreme turbulent heat fluxes events over the Gulf Stream [*Shaman et al.*, 2010]. For the South Pacific Ocean, *Qiu and Chen* [2006] and *Roemmich et al.* [2007] suggested that the 1990s decadal increase in sea surface height over the subtropical western basin of the South Pacific is related to a spin-up of the local subtropical ocean gyres. Based on long-term temperature and salinity observations from an ocean station off eastern Tasmania, *Ridgway* [2007] demonstrated that the East Australian Current has increased over the past 60 years. Based on repeated high-density XBT transects, CTD survey and satellite altimetry, *Ridgway et al.* [2008] also found a strengthening of the East Australian Current in the 1990s. Regarding the South Atlantic Ocean, *Goni et al.* [2011] observed a southward shift of the Brazil Current during 1993–2008 using
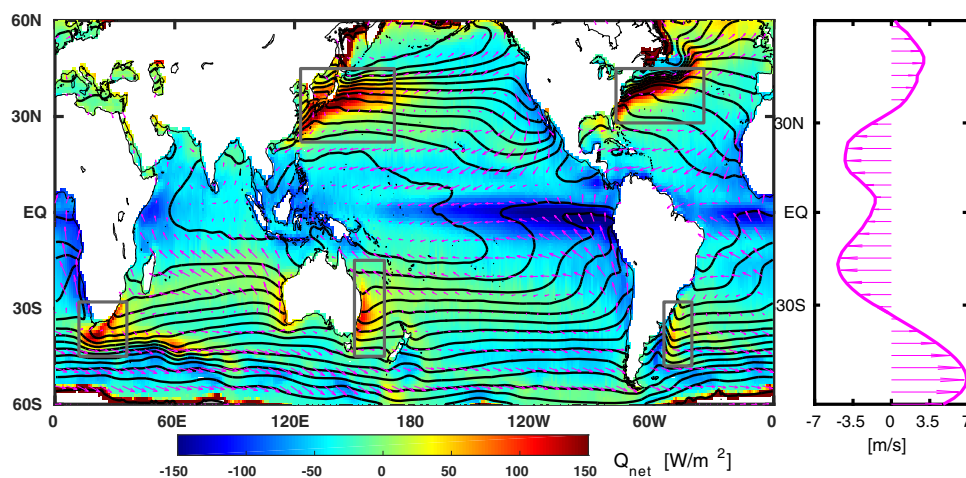
**Figure 1.** (left) Distribution of climatological $Q_{net}$ (shaded, positive upward), SST (black contours, contour interval is 2 K), and near-surface ocean winds (pink arrows). (right) Zonally averaged near-surface ocean zonal wind speeds (positive westerly). $Q_{net}$ is from the OAFlux/ ISCCP data set; SST is from the HadISST1 data set; near-surface ocean winds are based on the NCEP/NCAR. The overlaping periods 1984–2009 are selected to derive the climatological conditions.

satellite-derived sea height anomaly and sea surface temperature (SST). Over the Indian Ocean, the Agulhas leakage was reported to have increased due to latitudinal shifts in the Southern Hemisphere Westerlies [*Biastoch et al.*, 2009]. In addition, modeling studies indicate ocean circulation changes over the Southern Hemisphere in response to a positive trend of the Southern Annular Mode [*Hall and Visbeck*, 2002; *Cai et al.*, 2005; *Sen Gupta and England*, 2006; *Cai*, 2006; *Fyfe and Saenko*, 2006; *Sen Gupta et al.*, 2009]. These studies consistently show that the Southern Hemisphere subtropical gyres do shift southward as a consequence of a positive Southern Annular Mode.

Besides these studies focusing on individual branches of the WBCs, recent work suggests that the change over the WBCs is likely to be a global phenomenon over all ocean basins [*Wu et al.*, 2012; *Yang et al.*, 2016]. Based on multiple SST data sets, *Wu et al.* [2012] reported that a stronger warming trend occurred over the WBCs during the past century. They proposed that a synchronous poleward shift and/or intensification of WBCs were associated with the identified ocean surface warming [*Wu et al.*, 2012]. *Yang et al.* [2016] found that the ocean surface heat loss over the subtropical expansions of WBCs have increased, suggesting a stronger WBCs in the past half century. However, the confidence in WBCs dynamics changes is controversy due to the uncertainties and limitations of the data sets [*Brunke et al.*, 2002; *L'Ecuyer and Stephens*, 2003; *Van de Poll et al.*, 2006; *Gulev et al.*, 2007; *Krueger et al.*, 2013; *Dee et al.*, 2014]. Here, we use a wide range of independent data sets and metrics to evaluate the dynamic changes of WBCs.

WBCs transport large quantities of heat from the tropics to mid and high latitudes, and much of the heat is released along the routes of these currents. As shown in Figure 1, the meandering of WBCs can be clearly captured by the upward ocean surface heat flux. Following this idea, ocean surface heat flux is used as the main metric to identify the dynamic changes of WBCs.

The available ocean surface heat fluxes data sets have several potential sources of uncertainty (e.g., uncertainty in the flux computation algorithms, sampling issues, instrument biases, changing observation systems) [*Brunke et al.*, 2002; *L'Ecuyer and Stephens*, 2003; *Van de Poll et al.*, 2006; *Gulev et al.*, 2007]. Each data set has its own advantages and weaknesses. Satellite-blended records give observations with excellent spatial/temporal sampling, but they suffer from a lack of temporal coverage, which is insufficient to examine the long-term variability. Reconstructed and reanalysis products cover longer periods by synthesizing a variety of observations. However, the changing mix of observations can introduce spurious variability and trends into the output [*Dee et al.*, 2014]. The coupled general circulation models (CGCM) have the ability to simulate the Earth's climate over hundreds of years with consistent physical behaviors, but their performance on reproducing the climate variability is still under evaluation [*Refsgaard et al.*, 2014; *Bellucci et al.*, 2014]. For achieving reliable and comprehensive results, all three types of heat flux data sets mentioned above are included here. Moreover, the results based on sea surface heat flux will also be cross validated by the ocean velocity fields and ocean surface winds. Since the

**Table 1.** List of Data Sets Used in This Study

| Data Type | Data Name | Periods | References |
|---|---|---|---|
| Reconstructed | HadISST | 1870–2014 | *Rayner et al.* [2003] |
| Reconstructed | HadCRUT4 | 1850–2014 | *Morice et al.* [2012] |
| Satellite-blended | OISSTv2 | 1982–2014 | *Reynolds et al.* [2002] |
| Satellite-blended | OAFlux/ISCCP | 1983–2009 | *Rossow and Schiffer* [1991]; *Yu et al.* [2008] |
| Atmospheric reanalyses | NCEP/NCAR | 1948–2014 | *Kalnay et al.* [1996] |
| Atmospheric reanalyses | ERA40 | 1958–2001 | *Uppala et al.* [2005] |
| Atmospheric reanalyses | 20CRv2 | 1871–2012 | *Compo et al.* [2006, 2011] |
| Atmospheric reanalyses | ERA-20C | 1900–2010 | *Poli et al.* [2016] |
| Ocean reanalyses | ORA-S4 | 1958–2009 | *Balmaseda et al.* [2013] |
| Ocean reanalyses | SODA2.2.0 | 1948–2008 | *Carton and Giese* [2008] |
| Ocean reanalyses | GECCO | 1952–2001 | *Köhl and Stammer* [2008] |
| Ocean reanalyses | GECCO2 | 1948–2014 | *Köhl* [2015] |
| Climate model | CMIP5/historical | 1850–2005 | *Taylor et al.* [2012] |
| Climate model | CMIP5/RCP4.5 | 2006–2300 | *Taylor et al.* [2012] |

reliability of the data sets before the 1950s is still a subject of controversy [*Krueger et al.*, 2013], we focus our analysis on the period after 1958. The paper is organized as follows. In section 2, the data sets and methods used are briefly introduced. Section 3 presents the observed and simulated dynamic changes of the WBCs. The physical mechanism responsible for these changes is investigated in section 4. Discussion and conclusions are given in sections 5 and 6, respectively.

## 2. Data and Methodology

All the data sets used in this paper are listed in Table 1. The reconstructed SST from the Hadley Centre Global Sea Ice and Sea Surface Temperature v1 (HadISST1, 1870–2013) [*Rayner et al.*, 2003] is used to

**Table 2.** List of CMIP5 Models Used in This Study

| Model Name | Institutions |
|---|---|
| BCC-CSM1-1 | Beijing Climate Center, China Meteorological Administration |
| BNU-ESM | College of Global Change and Earth System Science, Beijing Normal University |
| CanESM2 | Canadian Centre for Climate Modelling and Analysis |
| CCSM4 | National Center for Atmospheric Research |
| CESM1-BGC | National Science Foundation, Department of Energy, National Center for Atmospheric Research |
| CESM1-CAM5 | National Science Foundation, Department of Energy, National Center for Atmospheric Research |
| CNRM-CM5 | Centre National de Recherches Meteorologiques/Centre Europeen de Recherche et Formation Avancees en Calcul Scientifique |
| CSIRO-Mk3.6.0 | Commonwealth Scientific and Industrial Research Organisation in collaboration with the Queensland Climate Change Centre of Excellence |
| FGOALS-g2 | LASG, Institute of Atmospheric Physics, Chinese Academy of Sciences; and CESS, Tsinghua University |
| FIO-ESM | The First Institute of Oceanography, SOA, China |
| GFDL-CM3 | Geophysical Fluid Dynamics Laboratory |
| GFDL-ESM2G | Geophysical Fluid Dynamics Laboratory |
| GFDL-ESM2M | Geophysical Fluid Dynamics Laboratory |
| GISS-E2-H | NASA Goddard Institute for Space Studies |
| GISS-E2-R | NASA Goddard Institute for Space Studies |
| HadGEM2-CC | Met Office Hadley Centre |
| HadGEM2-ES | Met Office Hadley Centre and Instituto Nacional de Pesquisas Espaciais |
| INM-CM4 | Institute for Numerical Mathematics |
| IPSL-CM5A-MR | Institut Pierre-Simon Laplace |
| IPSL-CM5B-LR | Institut Pierre-Simon Laplace |
| MIROC-ESM-CHEM | Japan Agency for Marine-Earth Science and Technology, Atmosphere and Ocean Research Institute (The University of Tokyo), and National Institute for Environmental Studies |
| MIROC5 | Atmosphere and Ocean Research Institute (The University of Tokyo), National Institute for Environmental Studies, and Japan Agency for Marine-Earth Science and Technology |
| MPI-ESM-LR | Max Planck Institute for Meteorology (MPI-M) |
| MPI-ESM-MR | Max Planck Institute for Meteorology (MPI-M) |
| MRI-CGCM3 | Meteorological Research Institute |
| NorESM1-ME | Norwegian Climate Centre |
| NorESM1-M | Norwegian Climate Centre |
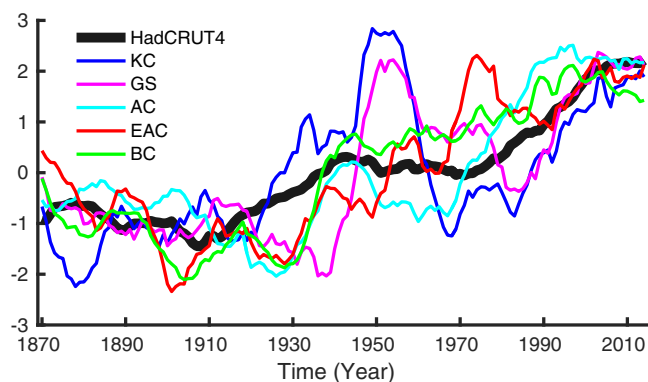
**Figure 2.** SST indices of WBCs (thin color line) and signal of global warming (Had-CRUT4, thick black line). All indices are standardized after applying an 11 year running mean. SST indices of WBCs are extracted using the following approach: First, regional mean SST indices are calculated over individual WBCs (as shown with grey rectangles in Figure 1, i.e., Kuroshio Current (KC), $123°E-170°E$, $22°N-45°N$; Gulf Stream (GS), $79°W-35°W$, $28°N-45°N$; Eastern Australian Current (EAC), $150°E-165°E$, $15°S-45°S$; Brazil Current (BC), $55°W-41°W$, $48°S-28°S$; Agulhas Current (AC), $12°E-36°E$, $45°S-28°S$). Then, the globally averaged SST anomaly is removed from the SST indices of individual WBCs.

compute the SST indices of individual WBCs. The time series of near surface temperature from the HadCRUT4 (1850–2013) [*Morice et al.*, 2012] is utilized to represent the signal of global warming.

Besides, two satellite-blended data sets are applied to identify the dynamic changes of WBCs. They are the SST from the Optimum Interpolation SST Analysis Version 2 (OISSTv2, 1982–2013) [*Reynolds et al.*, 2002], and the net surface heat flux ($Q_{net}$, sum of the radiative and turbulent heat fluxes) from the Objectively Analyzed Air-sea Fluxes and the International Satellite Cloud Climatology Project (OAFlux/ISCCP, 1983–2009) [*Rossow and Schiffer*, 1991; *Yu et al.*, 2008].

Moreover, two atmospheric reanalyses and four ocean reanalyses data sets are included, namely the National Centers for Environmental Prediction/National Center for Atmospheric Research reanalysis (NCEP/NCAR, 1948–2013) [*Kalnay et al.*, 1996], the European Centre for Medium-Range Weather Forecasts 40 year Reanalysis (ERA40, 1958–2001) [*Uppala et al.*, 2005], the European Centre for Medium-Range Weather Forecasts ocean reanalysis system 4 (ORA-S4, 1958–2009) [*Balmaseda et al.*, 2013], the Simple Ocean Data Assimilation (SODA2.2.0, 1948–2008) [*Carton and Giese*, 2008], and the German partner of the consortium for Estimating the Circulation and Climate of the Ocean (GECCO, 1952–2001, and GECCO2, 1948–2014) [*Köhl and Stammer*, 2008; *Köhl*, 2015].

Furthermore, the *historical* and Representative Concentration Pathway 4.5 (*RCP*4.5) simulations from the fifth phase of the Climate Model Intercomparison Project (CMIP5) [*Taylor et al.*, 2012] are used as well. Twenty-seven climate models are included to obtain the ensemble trends based on both *historical* and *RCP*4.5 simulations. Detailed information on the models we used here is summarized in Table 2.

Additionally, the results from the Twentieth Century Reanalysis (20CRv2) [*Compo et al.*, 2006, 2011] and the ECMWF's first atmospheric reanalysis of the 20th century (ERA-20C) [*Poli et al.*, 2016] are provided in the supporting information to further validate our results.

The data sets used in the present paper cover different time periods. For the reanalysis data sets, the overlapping period from 1958 to 2001 is selected. We examine the same time period (1958–2001) for the CMIP5 *historical* simulations and for the *RCP*4.5 simulations the time period of 2006–2100. As the CMIP5 models have different spatial resolutions and numbers of ensemble members, the trends in each CGCMs from the first ensemble member (named *r*1*i*1*p*1) [*Taylor et al.*, 2010] are computed first. Then the trends are regridded onto a regular $1°\times1°$ latitude-longitude grid using bilinear interpolation. Finally, they are averaged over all the corresponding simulations to get the multimodel ensemble trends. As the satellite-blended data sets cover relative short periods, the whole available time interval is utilized.

## 3. Dynamic Changes of WBCs

### 3.1. Results From Observations

Figure 2 shows the SST indices of the five WBCs after removing the globally averaged SST anomaly. Positive trends are observed, indicating that the ocean surface warming over the WBCs is outpacing other regions. Moreover, the SST indices of WBCs share similarities with the global warming signal. These features raise the question as to whether the strength of WBCs is affected by the global warming. It is also noticed that the SST indices of WBCs have strong decadal variations, especially for the Kuroshio Current and the Gulf Stream.
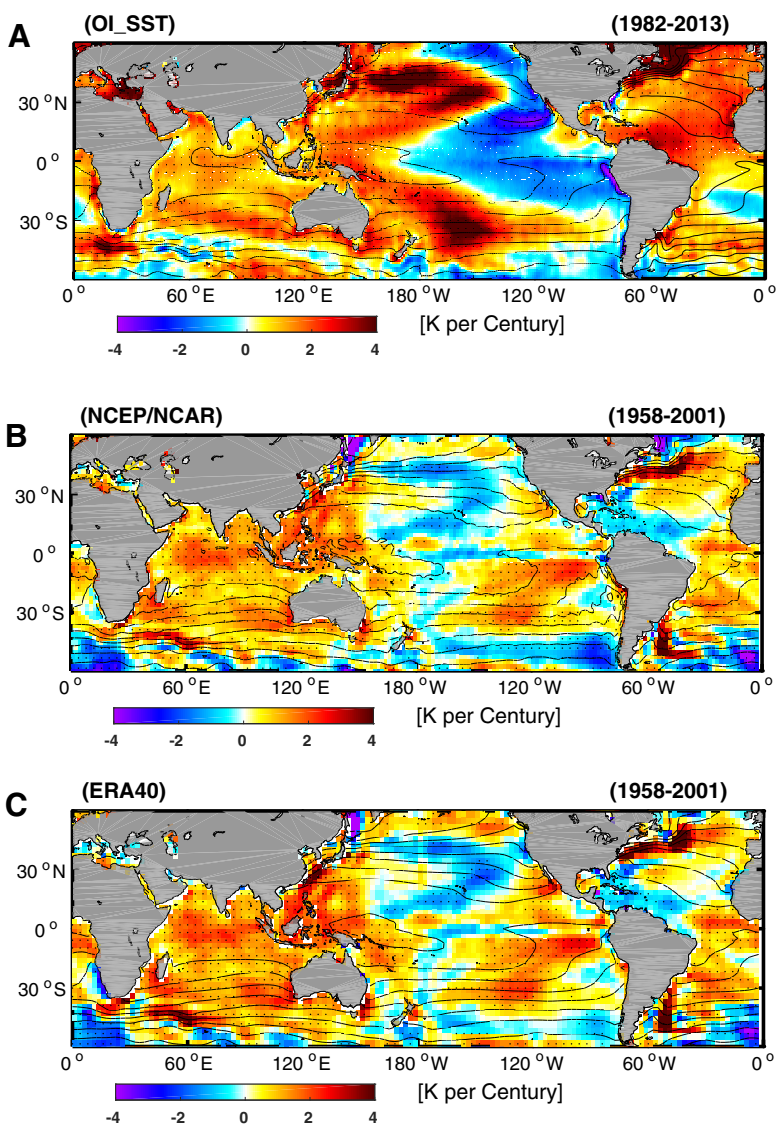
**Figure 3.** Observational trends in SST (shading). Black contours present climatological SST. Stippling indicates regions where the trends pass the 95% confidence level (Student's *t*-test).

The trends in SST and $Q_{net}$ (positive-upward) are depicted in Figures 3 and 4 (shading). The corresponding climatology values (contours) are also presented to locate the background routes of the WBCs.

The magnitudes and distributions of SST and $Q_{net}$ trends reveal discrepancies among different data sets over different time periods. In a relative short period of time, the satellite-blended data sets (OISSTv2 and OAFlux/ISCPP) mainly capture the signal of decadal climate variability, i.e., a negative phase of Pacific Decadal Oscillation [*Mantua et al.*, 1997] over the Pacific Ocean, and a positive phase of Atlantic Multidecadal Oscillation [*Schlesinger and Ramankutty*, 1994] over the Atlantic Ocean. Over a longer time scale, an overwhelming ocean surface warming is observed in the reanalysis data sets. Despite these discrepancies, consistent features emerge over the midlatitude expansions of the WBCs with substantial increase in both SST and $Q_{net}$. Such trends occur not only over individual WBCs, but for WBCs within all ocean basins. From a perspective of ocean-atmosphere heat balance, increased SST accompanied by enhanced ocean surface heat loss indicates that the ocean surface warming is not caused by the atmospheric forcing, but by an intensified ocean heat transport though the WBCs.

With respect to the regional features, we find that the trends are asymmetrical over different flanks of the WBCs. Both NCEP and ERA40 show a stronger increase in SST and $Q_{net}$ at the polar flanks of the Gulf Stream,
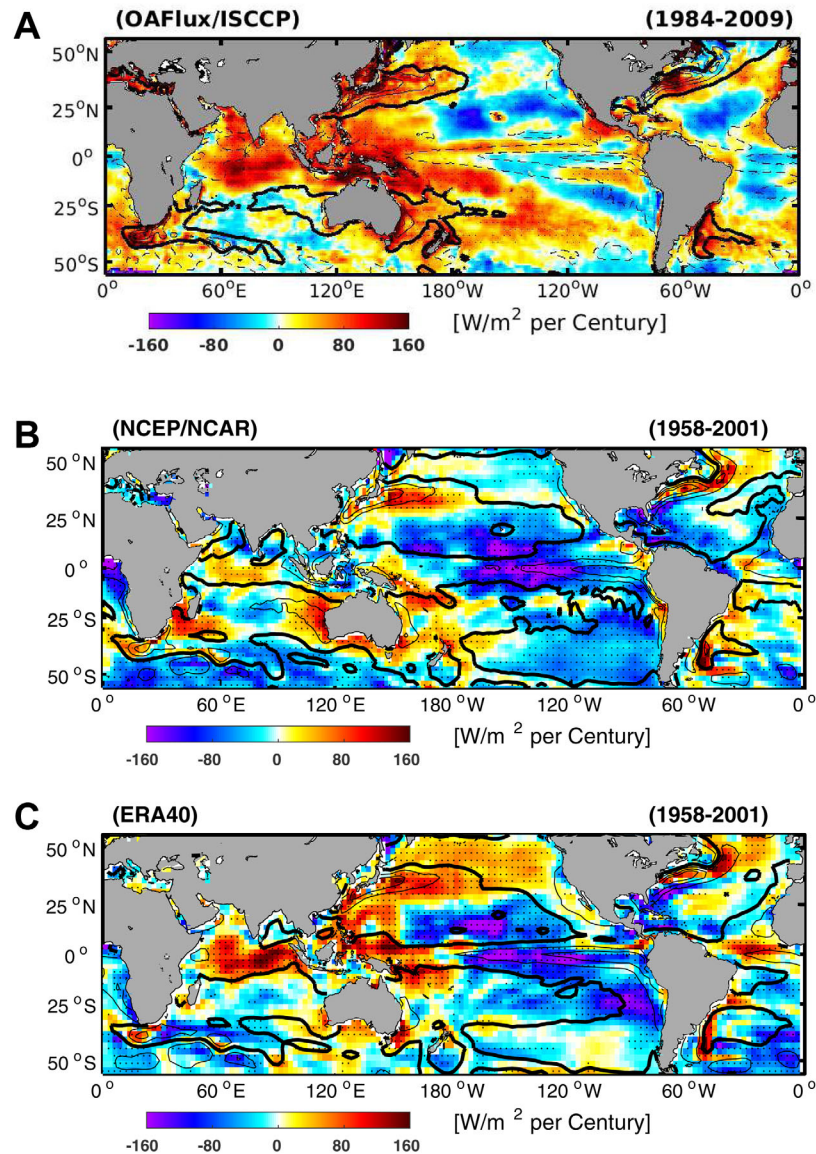
**Figure 4.** Observational trends in $Q_{net}$ (shading, positive-upward). Black contours present climatological $Q_{net}$. Upward $Q_{net}$ is in solid lines; downward $Q_{net}$ is in dashed lines; zero $Q_{net}$ is in bold lines. Stippling indicates regions where the trends pass the 95% confidence level (Student's *t*-test).

the Brazil Current, the East Australian Current, and the Agulhas Current. While, decreases or relative weaker increases in SST and $Q_{net}$ present themselves over the equator flanks of the above currents. The asymmetrical pattern reveals that the positions of the SST gradients and the high $Q_{net}$, induced by WBCs, are shifting toward the polar regions. However, one clear exception is found over the North Pacific Ocean, i.e., the Kuroshio Current, which experiences a stronger positive trend in $Q_{net}$ at the equatorial flank as illustrated by both reanalysis data sets, indicating an equatorward displacement of the Kuroshio Current over the period 1958–2001.

Comparing with the reanalysis data sets, the satellite-blended data sets also show stronger increases in $Q_{net}$ and SST over the polar flank of the Agulhas Current (Figures 3 and 4). While, due to their relatively short temporal period, the satellite-blended data sets are not able to identify signals of asymmetrical increases in the two elements over the other four WBCs.

In order to cross validate our results found from the ocean surface, we analyze the ocean velocity field. The imprint of the global warming on the ocean water velocity from four ocean reanalysis data sets is presented
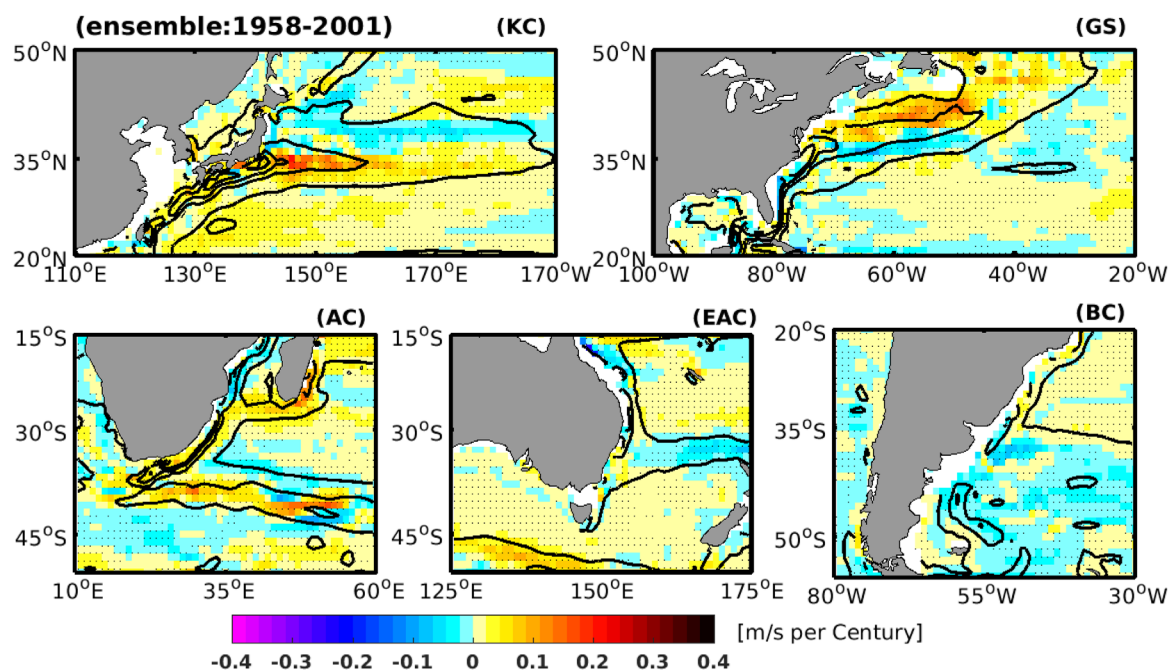
**Figure 5.** Ensemble trends in upper 100 m ocean velocity (shading) based on SODA, ORA-S4, GECCO, and GECCO2 ocean reanalyses. Contours: climatological depth-averaged (upper 100 m) sea water velocity. Stippling indicates areas where at least three data sets agree on the sign of the trends.

in the supporting information Figures S1–S4. Since the WBCs are strong ocean currents, the background ocean velocity field (contour lines) indicates the climatological paths. The shading gives the changes in velocity speed. These ocean reanalyses show large discrepancies in terms of regional patterns of WBCs changes. Even the same model system (GECCO and GECCO2) does not produce consistent results, mostly likely, due to high nonlinearity of the WBCs and insufficient number of ocean observations assimilated in the ocean reanalysis data sets. We show the ensemble mean change of upper ocean water velocity in Figure 5. Over the North Atlantic Ocean, a faster (slower) velocity over the polar (equator) flank of the Gulf Stream is observed, demonstrating a significant poleward shift of the Gulf Stream route. Over the southwestern Indian Ocean, there is a prominent positive trend of the Agulhas Current along the continental shelf of south-eastern Africa. In contrast, a reduced velocity is found at the route of the Agulhas Current in the Mozambique Channel, demonstrating that the Agulhas Current is stronger and shifting southward. For the Eastern Australian Current and the Brazil Current, the ensemble members (see supporting information Figures S1–S4) show large differences, which makes the ensemble mean meaningless. Nevertheless, the SODA data set shows an intensified and southward shift of both the Brazil Current and the Eastern Australian Current.

Over the North Pacific Ocean, we find that the Kuroshio Current is stronger and shifting toward the equator, which is again different from the other four WBCs. However, the results in the velocity field are in agreement with the observational $Q_{net}$ trends presented in the previous section (e.g., Figure 4).

### 3.2. Results From Climate Models

In this section, the dynamic changes of the WBCs are assessed on the basis of *historical* and *RCP*4.5 simulations from CMIP5 archives (Figures 6–9, respectively). In order to suppress the internal fluctuations, we analyze the ensemble mean of 27 climate models. In general, the climate models present very similar patterns of WBCs climate changes over the Southern Hemisphere in comparison with observations. Over the Agulhas Current, the East Australian Current and the Brazil Current, the location of the maximum SST increase is found over the polar flanks of their midlatitude expansions. Meanwhile, a relatively weak SST increase is found over their equatorial flanks. The corresponding $Q_{net}$ trend exhibits dipole modes (positive values at the polar flank and negative values at the equator flank) over their midlatitude expansions. Also, the ocean
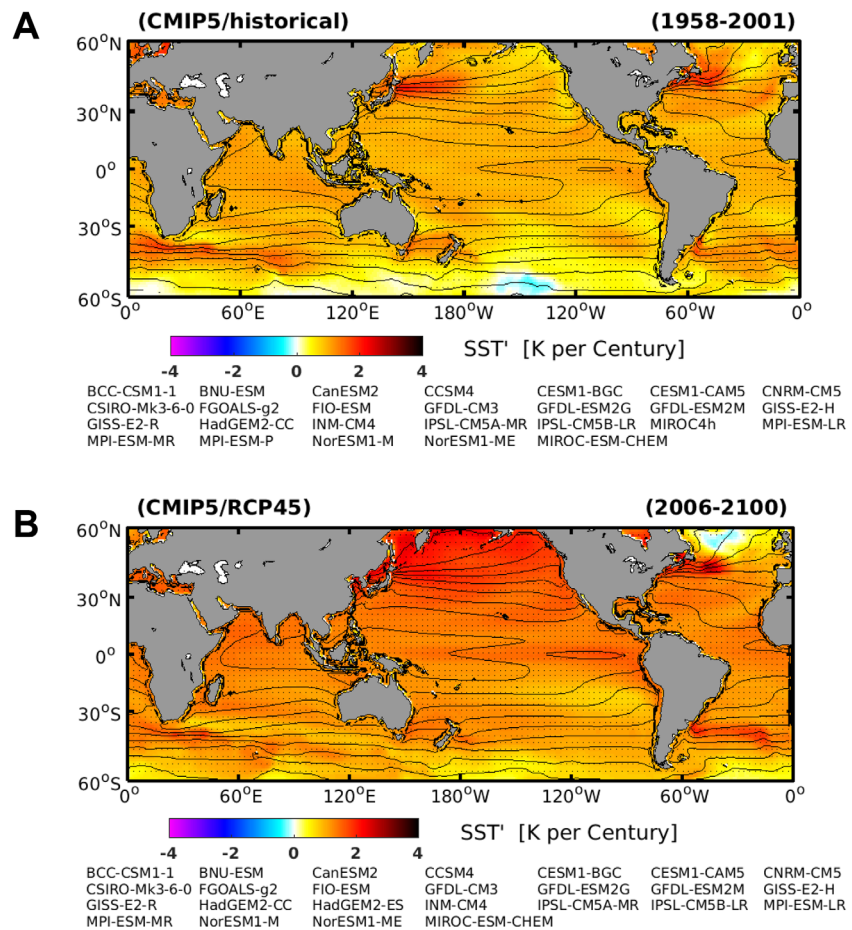
**Figure 6.** Multimodel ensemble trends in SST (shading) based on the *historical* and *RCP*4.5 simulations. Black contours present climatological SST. The models used to estimate the ensemble values are listed below each plot. Stippling indicates areas where at least 2/3 of the models agree on the sign of the trends.

velocity trends over the above WBCs consistently illustrate increasing and poleward shifting of these currents.

Due to the large internal variability of the Northern Hemisphere WBCs (Figure 2), there are strong discrepancies between the observations and climate models, e.g., the strengthening and poleward shift of the Kuroshio Current and a significant weakening Gulf Stream, with reducing $Q_{net}$ and decreasing ocean velocity (Figures 6–9).

We notice that the ensemble results in the *historical* simulations are less pronounced compared to the *RCP*4.5 simulations, because the global warming signal in the *historical* simulations is not beyond the model internal variability.

## 4. Possible Mechanism

The easterly winds over low latitudes, associated with the westerly winds over high latitudes, largely drive the anticyclonic subtropical ocean gyres, which show an intensification over the western boundary (Figure 1) [*Pedlosky*, 1996]. Significant dynamic changes of WBCs hint that the near-surface ocean zonal wind may have changed.

Figures 10 and 11 show the trends of the near-surface ocean zonal winds in the observational data sets and CMIP5 simulations, respectively. Over the Southern Hemisphere, the wind trends over the mid and high latitudes are dominated by stronger westerly winds. Meanwhile, stronger easterly winds are found over most of the subtropical regions. Such trends reinforce the background zonal winds. As a consequence, the wind
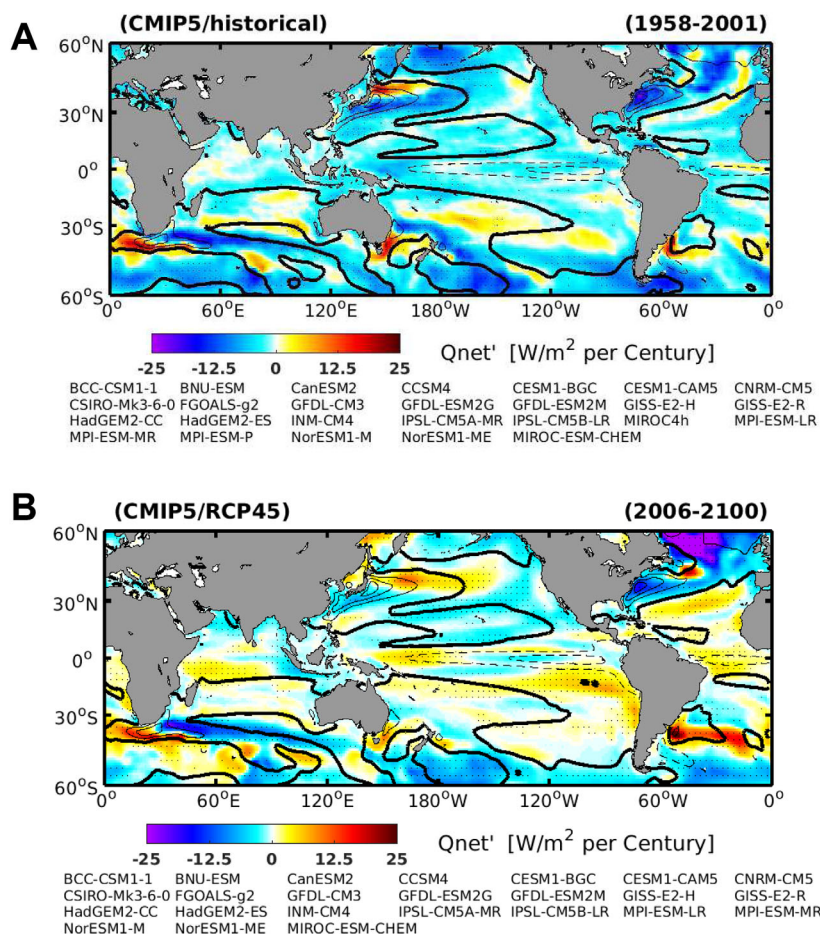
**Figure 7.** Multimodel ensemble trends in $Q_{net}$ (shading) based on the *historical* and *RCP*4.5 simulations. Black contours present climatological $Q_{net}$. Upward $Q_{net}$ is in solid lines; downward $Q_{net}$ is in dashed lines; zero $Q_{net}$ is in bold lines. The models used to estimate the ensemble values are listed below each plot. Stippling indicates areas where at least 2/3 of the models agree on the sign of the trends.

shear between the low and the high latitudes (wind stress curl) becomes stronger, which can force stronger WBCs in a warming climate. Besides the intensification of the zonal wind, all data sets consistently show that the zonal mean winds are shifting toward the South Pole in comparison with their climatology profile (Figures 10 and 11, right-side). Such shifts show dynamic consistency with the poleward shift of the Southern Hemisphere WBCs.

Over the North Atlantic, all the data sets consistently show a stronger and poleward shift of zonal wind. However, over North Pacific, some discrepancies appear between the observations (1958–2001) and climate models. Both atmospheric reanalyses present a stronger and equatorward shift of the North Pacific westerlies during 1958–2001, which contribute to a stronger and equatorward shift of the Kuroshio Current, (section 3.1). In contrast, the CMIP5 models simulate stronger and poleward shift of the North Pacific westerlies, forcing a stronger and poleward shift of the Kuroshio Current, as identified in section 3.2. To explore the reason for the differences over Northern Pacific, we present the long-term (1900–2010) trends of surface wind based on the century long reanalyses (supporting information Figure S5). Both 20CRv2 and ERA-20C consistently presents a stronger and poleward shift of the Northern Pacific westerly, indicating the observed equatorward shift during 1958–2001 are attribute to internal variability, as also shown in Figure 2.

Associated with the near-surface wind, the SLP trends are displayed in Figures 12 and 13, respectively. Both the observations as well as the CMIP5 models consistently show a decreasing SLP over the Poles and increasing SLP over midlatitudes of both Hemispheres. It is worth noting that the results based on the 20CRv2 and ERA-20C (supporting information Figure S6) resemble the patterns as we have identified here.
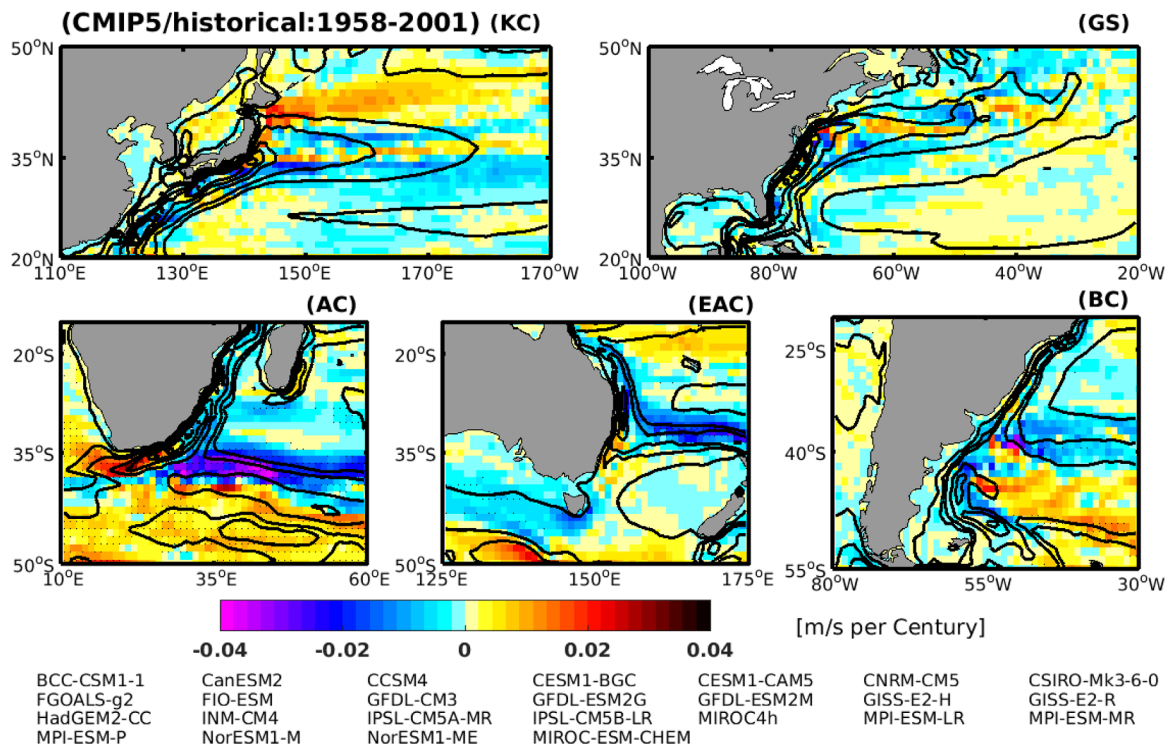
**Figure 8.** Multimodel ensemble trends in upper 100 m ocean velocity (shading) based on the *historical* simulations. Contours: climatological depth-averaged (upper 100 m) sea water velocity. The models used to estimate the ensemble values are listed in the low part of the corresponding plots. Stippling indicates areas where at least 2/3 of the models agree on the sign of the trends.
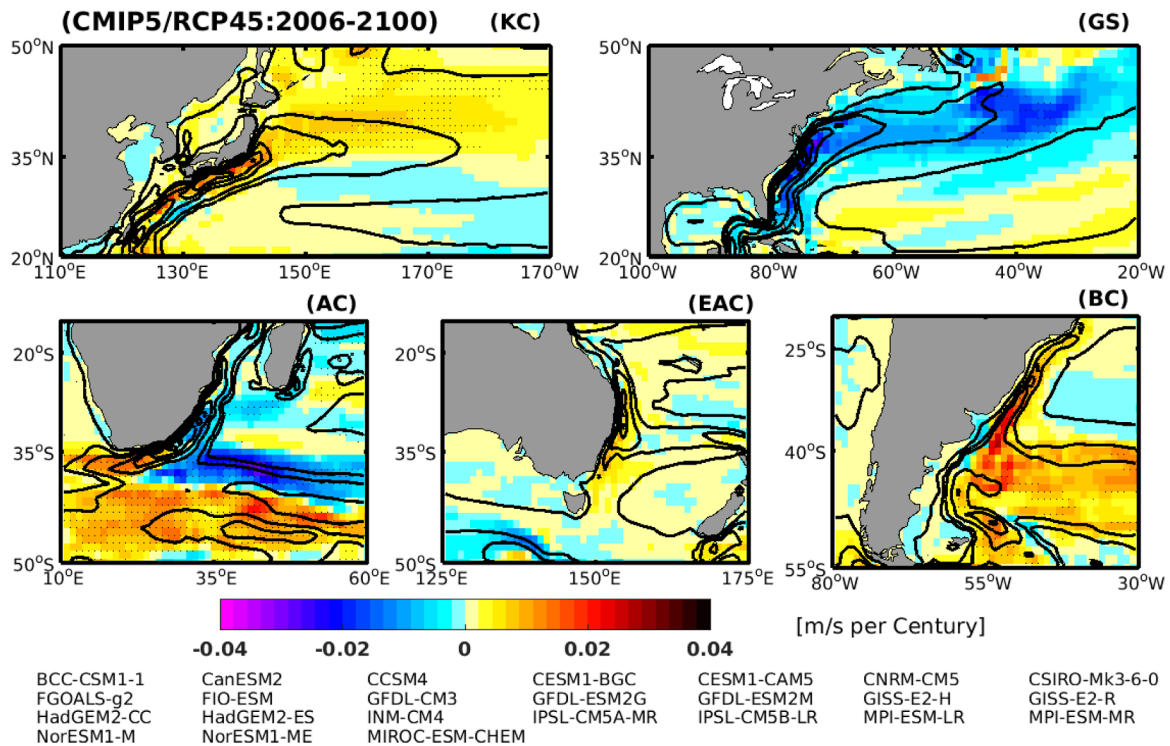


**Figure 9.** Multimodel ensemble trends in upper 100 m ocean velocity (shading) based on the *RCP*4.5 simulations. Contours: climatological depth-averaged (upper 100 m) sea water velocity. The models used to estimate the ensemble values are listed below each plot. Stippling indicates areas where at least 2/3 of the models agree on the sign of the trends.
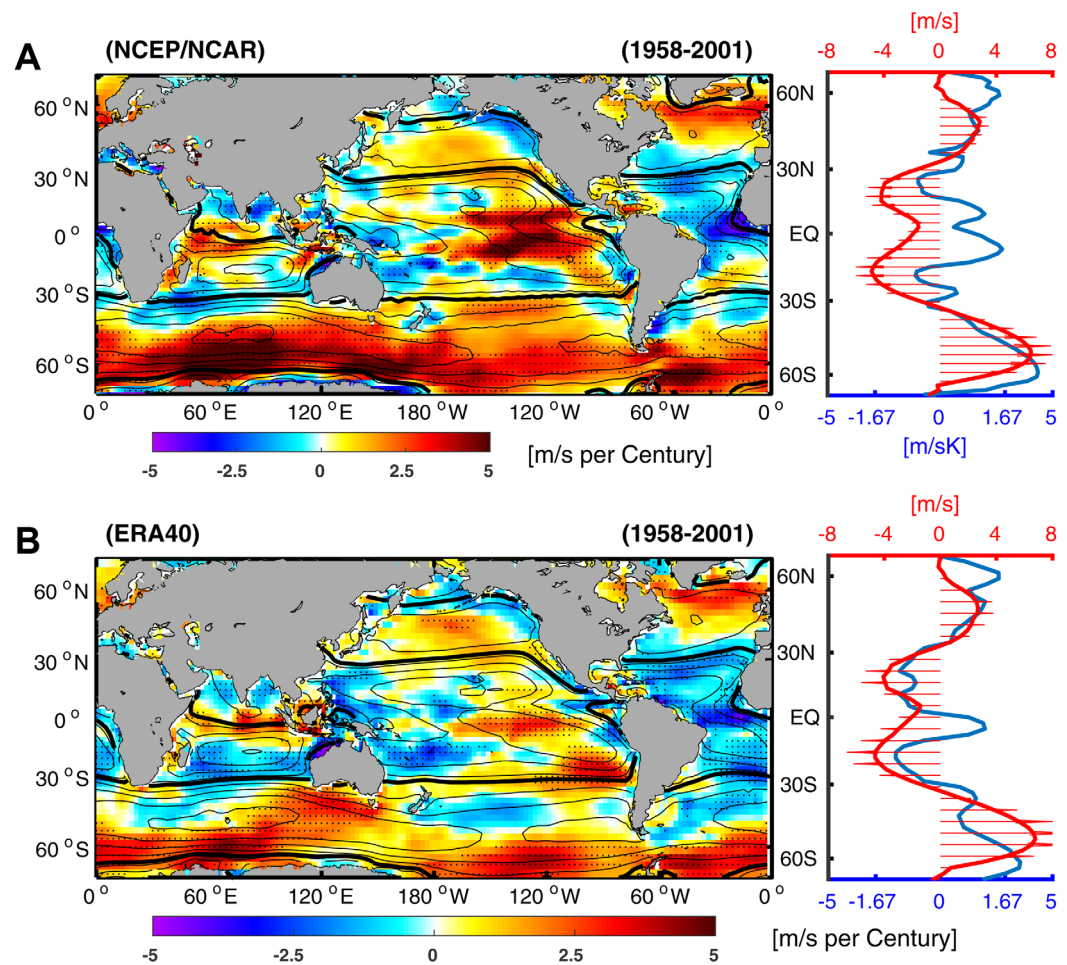
**Figure 10.** (left) Trends (shaded) and climatology (contours) near-surface ocean zonal wind. Easterly winds are in solid lines; westerly winds are in dashed lines; zero zonal winds are bold. Stippling indicates regions where the trends pass the 95% confidence level (Student's *t*-test). (right) Zonally averaged trend (blue) and climatology (red with arrow) of near-surface ocean zonal winds. Results are based on the NCEP/NCAP and ERA40 atmospheric reanalyses.

The near-surface ocean zonal wind and SLP show similar features as the positive phase of the annular modes (Northern Annular Mode (NAM) and Southern Annular Mode (SAM)), which are characterized by stronger and poleward shifts of the westerly winds, associated with negative SLP anomalies over high latitudes and positive SLP anomalies over midlatitudes. We propose that the positive annular mode-like trends contribute to the intensification of the near-surface ocean zonal winds and to shift them poleward. The changing winds force a strengthening and poleward displacement of the WBCs. As a result, more heat is transported from the tropics to the mid and high latitudes, which could significantly increase the SST and ocean heat loss ($Q_{net}$) there. Moreover, as the routes of the WBCs are shifting poleward, the position of the high $Q_{net}$ over the WBCs will also shift poleward.

## 5. Discussion

*Wu et al.* [2012] found an enhanced warming over the WBCs. They investigated the mechanism based on two century-long reanalyses data sets, the 20CRv2 and the Simple Ocean Data Assimilation (SODA) [*Giese and Ray*, 2011]. However, the detection of the WBCs dynamics changes is challenging due to limited observations and the uncertainties in the data sets [*Wu et al.*, 2012; *Stocker et al.*, 2013]. To further explore this, we use more independent data sets and more metrics to identify and explain the dynamic changes of WBCs. The common features among these broad ranges of data resources indicate that the WBCs (except the Gulf Stream) are strengthening and shifting toward the poles in a warming climate.
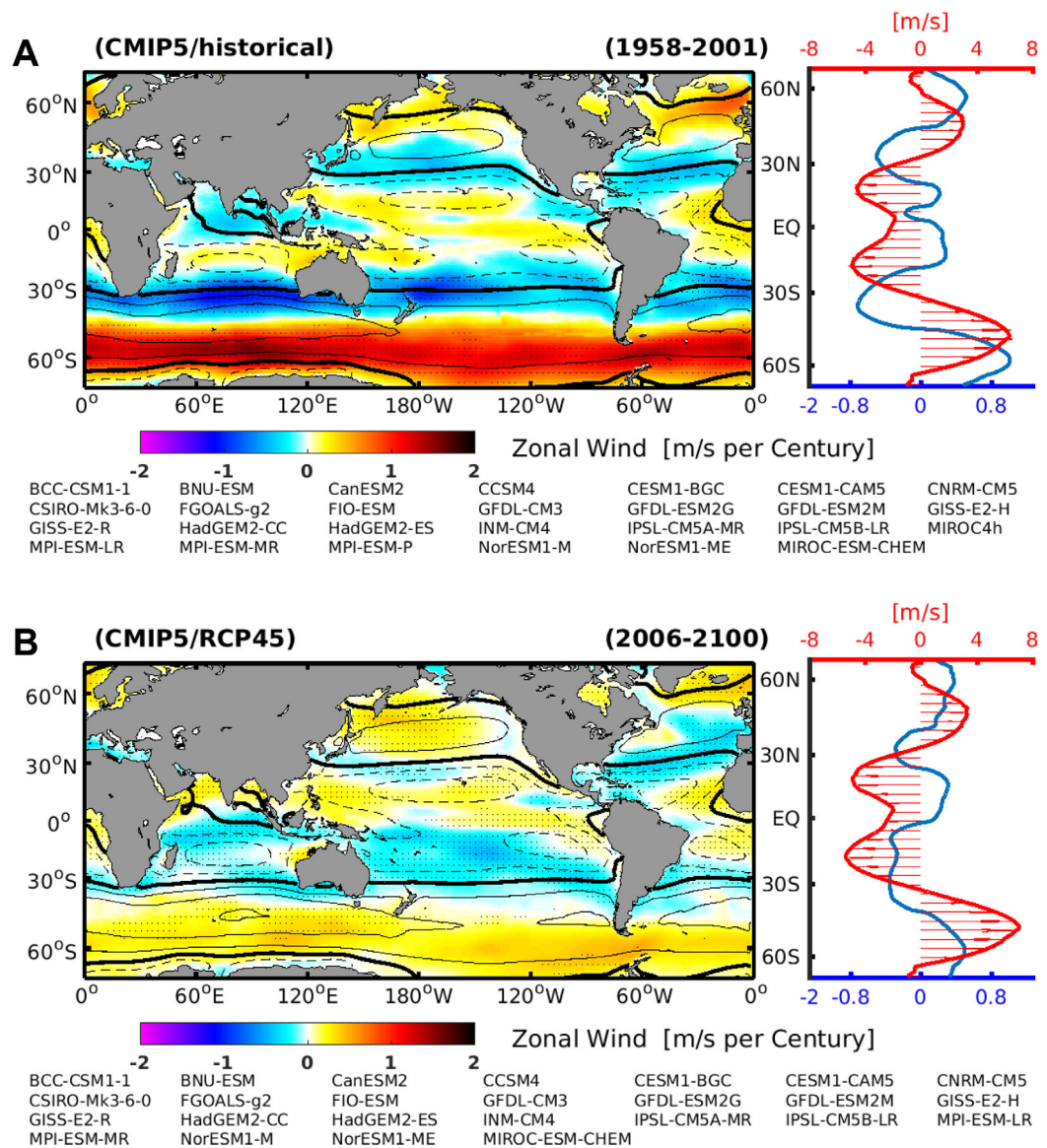
**Figure 11.** (left) Multimodel ensemble trends (shaded) and climatology (contours) near-surface ocean zonal wind. Easterly winds are in solid lines; westerly winds are in dashed lines; zero zonal winds are bold. Stippling indicates areas where at least 2/3 of the models agree on the sign of the trends. (right) Zonally averaged trend (blue) and climatology (red with arrow) of near-surface ocean zonal winds. Results are based on the *historical* and *RCP4.5* simulations. The models used to estimate the ensemble values are listed below each plot.

Over the Southern Hemisphere, observational data and climate models show consistent results. However, over the Northern Hemisphere, the observed Gulf Stream and Kuroshio Current have strong decadal variations, as shown in Figure 2. Observations (climate models) record an equatorward (poleward) shift of the Kuroshio Current over the period 1958–2001. *Seager et al.* [2001]; *Taguchi et al.* [2007]; *Sasaki and Schneider* [2011] demonstrated that the 1976/1977 equatorward shift in basin-scale winds contributed to the corresponding movement of the Kuroshio Current. However, from a long-term perspective (1900–2010), both 20CRv2 and ERA-20C present a poleward shift of surface wind over the Pacific Ocean (supporting information Figure S5), indicating the observed equatorward shift of Kuroshio Current over the period 1958–2001 is likely to be due to natural climate variations. Over the North Atlantic Ocean, the observations during 1958–2001 present a stronger and poleward shift of the Gulf Stream (consistent with the surface wind), while the climate models show a weakening of the Gulf Stream in response to global warming. The Gulf Stream is part of the upper branch of the Atlantic Meridional Overturning Circulation (AMOC). Strength of the Gulf Stream is determined not only by the near-surface ocean wind, but also by the AMOC, particularly on
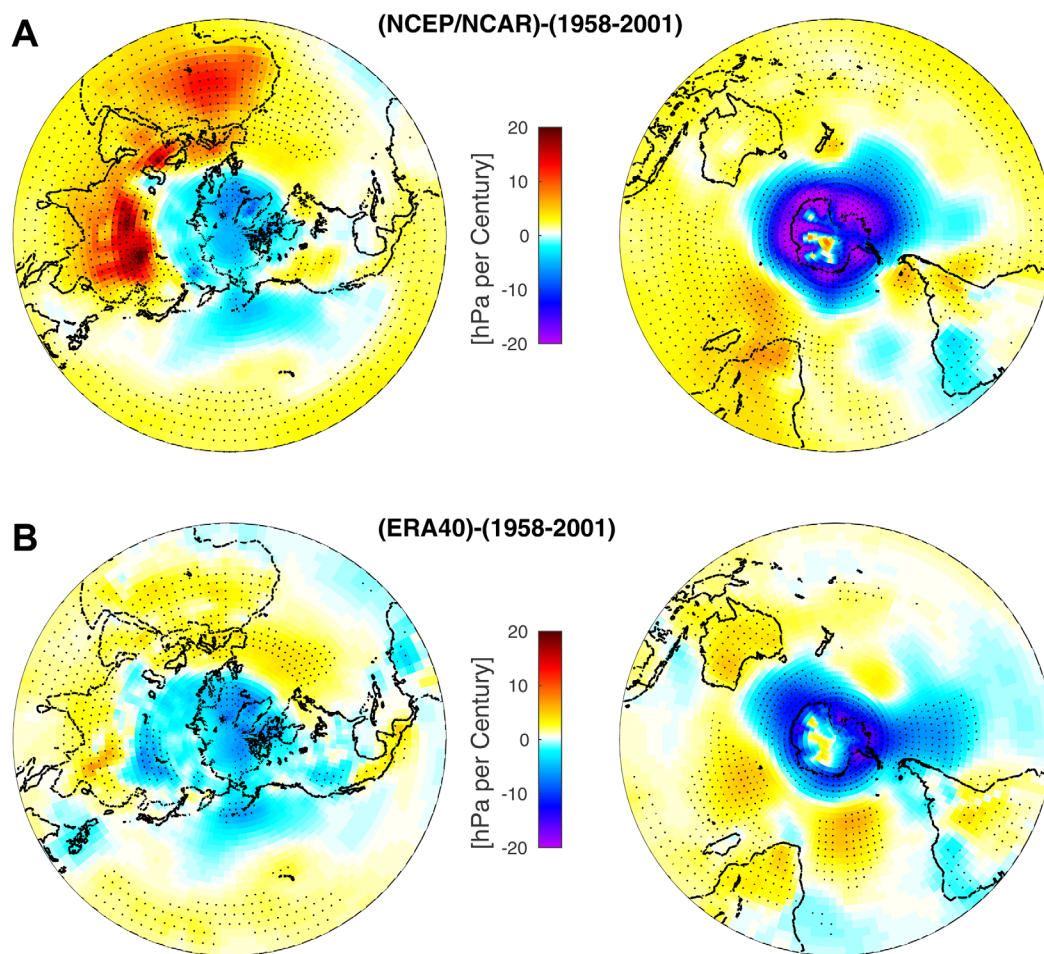
**Figure 12.** Trends in SLP based on the NCEP/NCAR and ERA40 data sets, respectively. Stippling indicates regions where the trends pass the 95% confidence level (Student's *t*-test).

multidecadal and centennial time scales. The simulated weakening of AMOC [e.g., *Lohmann et al.*, 2008; *Cheng et al.*, 2013] is likely linked to the weakening Gulf Stream.

Regarding the potential driving mechanism, several previous studies have focused on the local climate feedback. *Sakamoto et al.* [2005] have investigated the responses of the Kuroshio Current to global warming and suggested that a strengthening of the Kuroshio Current is caused by an El Niño-like mode. Indeed, the climate phenomenon over the Pacific Ocean (i.e., ENSO, PDO) plays a vital role in the variability of the Kuroshio Current, particularly on interannual to decadal time scales [*Qiu*, 2003; *Qiu and Chen*, 2005; *Taguchi et al.*, 2007; *Andres et al.*, 2009; *Sasaki and Schneider*, 2011]. However, we found that the common features of WBCs changes are characterized by an intensification and a poleward shift. Such changes are not an isolated phenomenon over individual ocean basins, but a global effect. Thus, the dynamic changes of the WBCs should be caused by a factor that can influence all ocean basins, such as we proposed, the positive annular mode-like trends over both hemispheres. Previously, the typical features of the annular modes in the wind field are described as an intensification and poleward shift of the westerly winds [*Thompson and Wallace*, 2000]. Here, we suggest that both the easterly winds over the low latitudes and the westerly winds over the mid and high latitudes have strengthened. Meanwhile, the profile of the zonal winds is shifting poleward over both hemispheres. The systematic changes in zonal winds are consistent with the poleward shift of the Hadley Cell [*Hu and Fu*, 2007; *Lu et al.*, 2007; *Johanson and Fu*, 2009], the expansion of the tropical belt [*Santer et al.*, 2003; *Seidel and Randel*, 2007; *Seidel et al.*, 2007; *Fu and Lin*, 2011], and the poleward shift of the subtropical dry zones [*Previdi and Liepert*, 2007].
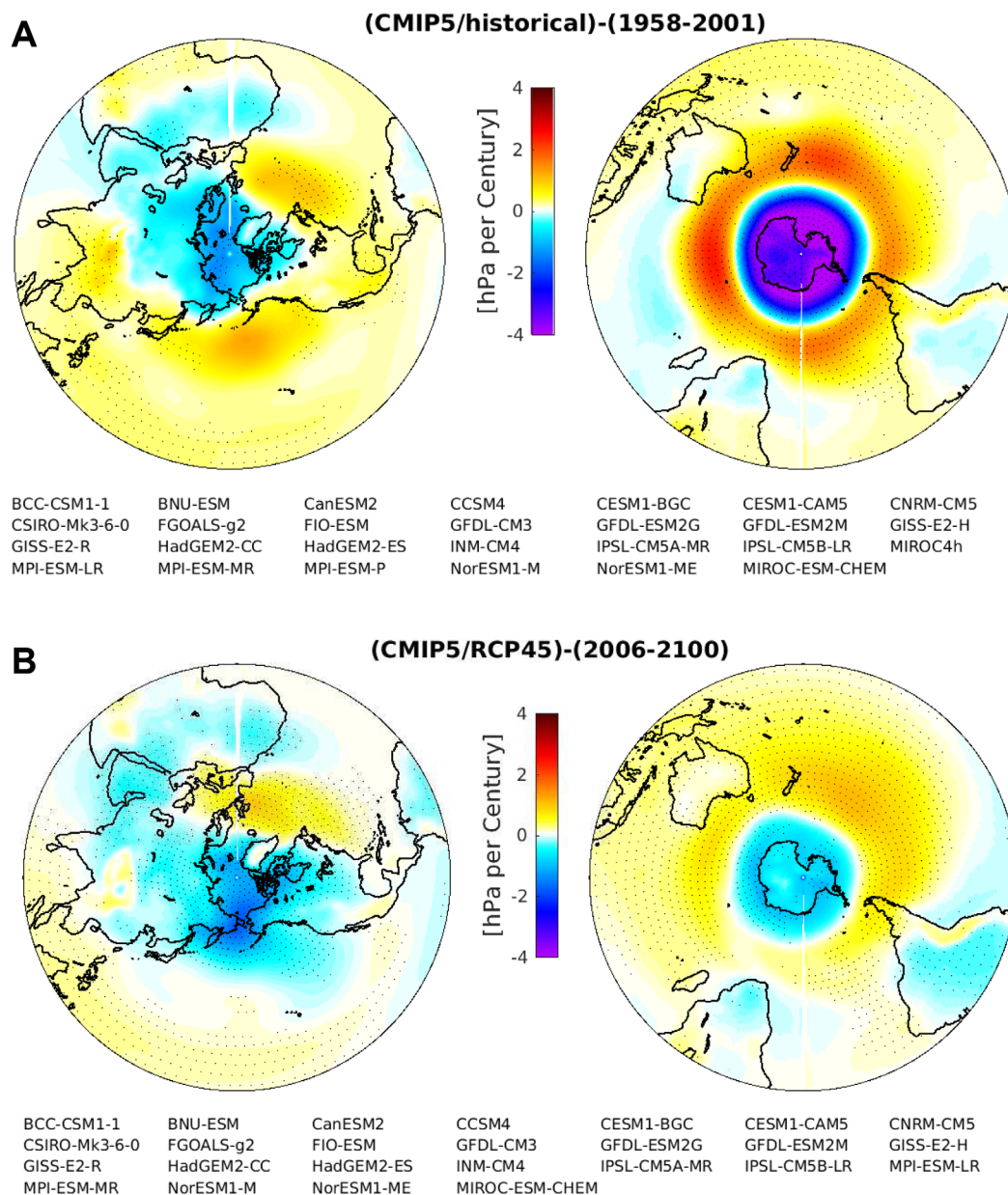
**Figure 13.** Multimodel ensemble trends in SLP based on the *historical* and *RCP*4.5 simulations. The models used to estimate the ensemble values are listed below each plot. Stippling indicates areas where at least 2/3 of the models agree on the sign of the trends.

For the Northern Hemisphere, *Sato et al.* [2006] demonstrated that the Arctic Oscillation-like trends are responses to a northward shift of the subtropical wind-driven gyre in the North Pacific Ocean. *Curry and McCartney* [2001] proved that the transport of the Gulf Stream has intensified due to a stronger North Atlantic Oscillation after the 1960s. Their conclusions are in agreement with ours, because the North Atlantic Oscillation and the Arctic Oscillation (or NAM) show very similar evolutions [*Deser*, 2000; *Rogers and McHugh*, 2002; *Feldstein and Franzke*, 2006]. Observations show a stronger NAM during the past several decades. However, a weaker NAM from the late 1990s is observed [*Thompson and Wallace*, 2000] simultaneously with the global warming hiatus [*Easterling and Wehner*, 2009]. Several factors are suggested having impact on the variations of NAM, i.e., the greenhouse gases, the stratosphere-troposphere interaction, local sea ice variability, and remote tropical influence [*Fyfe et al.*, 1999; *Wang and Chen*, 2010; *Gillett and Fyfe*, 2013; *Cattiaux and Cassou*, 2013]. The trend in Northern Annular Mode during 1958–2001 is most likely dominated by its natural variations. However, for a longer-time period, both the century-long atmosphere reanalyses (i.e.,

20CRv2 and ERA-20C in supporting information Figures S5 and S6) and the CMIP5 climate models illustrate that the NAM is propagating to a positive phase under global warming.

Over the Southern Hemisphere, several studies have also confirmed that the Southern Hemisphere subtropical gyres are influenced by the SAM [*Hall and Visbeck*, 2002; *Cai et al.*, 2005; *Sen Gupta and England*, 2006; *Cai*, 2006; *Fyfe and Saenko*, 2006; *Sen Gupta et al.*, 2009]. Both observations [*Thompson and Wallace*, 2000; *Marshall*, 2003] and CGCM simulations [*Fyfe et al.*, 1999; *Stone et al.*, 2001; *Kushner et al.*, 2001; *Cai et al.*, 2003; *Gillett and Thompson*, 2003; *Rauthe et al.*, 2004; *Arblaster and Meehl*, 2006; *Gillett and Fyfe*, 2013] show that the SAM is entering a positive phase. The ozone depletion was suggested to be the main driver for the observed positive trend of SAM [*Thompson and Solomon*, 2002; *Kindem and Christiansen*, 2001; *Sexton*, 2001; *Gillett and Thompson*, 2003; *Thompson et al.*, 2011; *Polvani et al.*, 2011]. However, increasing greenhouse gases were also suggested to have a contribution on it [*Fyfe et al.*, 1999; *Kushner et al.*, 2001; *Cai et al.*, 2003; *Rauthe et al.*, 2004]. As it is shown in Figures 11 and 13, a stronger SAM trend is found during 1958–2001 when both the ozone depletion and the increasing greenhouse gas force the SAM. However, in the near future, as ozone levels recover, it will play an oppose role as increasing greenhouse gas. The positive trend in SAM might be weaker or reverse sign over the coming decades [*Arblaster et al.*, 2011].

WBCs have a broad impact on the climate and economy over the adjacent mainland, e.g., the temperature, fishing, storms, precipitation, and extreme climate events [*Seager et al.*, 2002; *Cai et al.*, 2005; *Minobe et al.*, 2008]. As expected, stronger WBCs will increase the atmospheric baroclinicity, favoring more storms [*Shaman et al.*, 2010]. Moreover, the adjacent regions of the WBCs suffer more warming than other regions, due to the increased heat transport by the WBCs, especially over Eastern Asian, where the Kuroshio Current transports much more heat [*Tang et al.*, 2009]. In contrast, a weakening of the Gulf Stream in this century can reduce the heat release from the ocean, and contribute to a relative cooling over Europe and Eastern America, a feature suggested by *Dima and Lohmann* [2010] and *Rahmstorf et al.* [2015]. We suggest that particular attention must be paid to the climate change over the adjacent regions of WBCs.

## 6. Conclusions

We find observational and model support for an intensification and poleward movement of WBCs in response to anthropogenic climate change. The one exception to this is the Gulf Stream where a weakening of the AMOC tends to reduce the strength of the Gulf Stream. Elsewhere the intensification and poleward shift are postulated to be driven by a stronger and poleward shift of the extratropical winds and expansion of the Hadley Cell. In the Southern Hemisphere, the observed record indicates this intensification and southward shift is already occurring perhaps because ozone depletion and rising greenhouse gas have worked in the same direction in forcing a positive SAM. In the Northern Hemisphere, natural variability appears to be temporarily interrupting the poleward shift of the Kuroshio and have driven a poleward shift of the Gulf Stream via the upward trend in the Arctic Oscillation over the analyzed period (1958–2001). As the 21st century progresses, we expect the poleward shift in the Northern Hemisphere to become clearer as the response to radiative forcing grows in size relative to the natural variability. In the Southern Hemisphere, changes in intensity and latitude of the WBCs will depend on the opposing impacts of ozone recovery, rising greenhouse gas, and the varying influence of natural variability. In all cases, the dynamic changes of the WBCs impact poleward ocean heat transport, regional climate, storm tracks, and ocean ecosystems. So, improved understanding and projection of how they will evolve is an important area of research to which the current work hopefully provides a useful impetus.

## References

Andres, M., J.-H. Park, M. Wimbush, X.-H. Zhu, H. Nakamura, K. Kim, and K.-I. Chang (2009), Manifestation of the Pacific decadal oscillation in the Kuroshio, *Geophys. Res. Lett.*, *36*, L16602, doi:10.1029/2009GL039216.

Arblaster, J. M., and G. A. Meehl (2006), Contributions of external forcings to southern annular mode trends, *J. Clim.*, *19*(12), 2896–2905.

Arblaster, J. M., G. Meehl, and D. Karoly (2011), Future climate change in the southern hemisphere: Competing effects of ozone and greenhouse gases, *Geophys. Res. Lett.*, *38*, L02701, doi:10.1029/2010GL045384.

Balmaseda, M. A., K. Mogensen, and A. T. Weaver (2013), Evaluation of the ECMWF ocean reanalysis system ORAS4, *Q. J. R. Meteorol. Soc.*, *139*(674), 1132–1161.

Bellucci, A., et al. (2014), An assessment of a multi-model ensemble of decadal climate predictions, *Clim. Dyn.*, *44*(9-10), 2787–2806.

Biastoch, A., C. W. Böning, F. U. Schwarzkopf, and J. Lutjeharms (2009), Increase in Agulhas leakage due to poleward shift of Southern Hemisphere westerlies, *Nature*, *462*(7272), 495–498.

Brunke, M. A., X. Zeng, and S. Anderson (2002), Uncertainties in sea surface turbulent flux algorithms and data sets, *J. Geophys. Res.*, *107*(C10), 3141, doi:10.1029/2001JC000992.

Cai, W. (2006), Antarctic ozone depletion causes an intensification of the Southern Ocean super-gyre circulation, *Geophys. Res. Lett.*, *33*, L03712, doi:10.1029/2005GL024911.

Cai, W., P. H. Whetton, and D. J. Karoly (2003), The response of the Antarctic Oscillation to increasing and stabilized atmospheric CO2, *J. Clim.*, *16*(10), 1525–1538.

Cai, W., G. Shi, T. Cowan, D. Bi, and J. Ribbe (2005), The response of the Southern Annular Mode, the East Australian Current, and the southern mid-latitude ocean circulation to global warming, *Geophys. Res. Lett.*, *32*, L23706, doi:10.1029/2005GL024701.

Carton, J. A., and B. S. Giese (2008), A reanalysis of ocean climate using Simple Ocean Data Assimilation (SODA), *Mon. Weather Rev.*, *136*(8), 2999–3017.

Cattiaux, J., and C. Cassou (2013), Opposite CMIP3/CMIP5 trends in the wintertime Northern Annular Mode explained by combined local sea ice and remote tropical influences, *Geophys. Res. Lett.*, *40*, 3682–3687, doi:10.1002/grl.50643.

Cheng, W., J. C. Chiang, and D. Zhang (2013), Atlantic Meridional Overturning Circulation (AMOC) in CMIP5 Models: RCP and Historical Simulations, *J. Clim.*, *26*(18), 7187–7197.

Colling, A. (2001), *Ocean Circulation*, vol. 3, Butterworth-Heinemann, Oxford, U. K.

Compo, G. P., J. S. Whitaker, and P. D. Sardeshmukh (2006), Feasibility of a 100-year reanalysis using only surface pressure data, *Bull. Am. Meteorol. Soc.*, *87*(2), 175–190.

Compo, G. P., et al. (2011), The twentieth century reanalysis project, *Q. J. R. Meteorol. Soc.*, *137*(654), 1–28.

Cronin, M. F., et al. (2010), "Monitoring Ocean - Atmosphere Interactions in Western Boundary Current Extensions" in *Proceedings of Ocean-Obs'09: Sustained Ocean Observations and Information for Society* (Vol. 2), Venice, Italy, 21–25 September 2009, edited by Hall, D. E. Harrison, and D. Stammer, ESA Publication WPP-306, doi:10.5270/OceanObs09.cwp.20.

Curry, R. G., and M. S. McCartney (2001), Ocean gyre circulation changes associated with the North Atlantic Oscillation, *J. Phys. Oceanogr.*, *31*(12), 3374–3400.

Dee, D., M. Balmaseda, G. Balsamo, R. Engelen, A. Simmons, and J.-N. Thépaut (2014), Toward a consistent reanalysis of the climate system, *Bull. Am. Meteorol. Soc.*, *95*(8), 1235–1248.

Deser, C. (2000), On the teleconnectivity of the" Arctic Oscillation," *Geophys. Res. Lett.*, *27*(6), 779–782.

Deser, C., M. Alexander, and M. Timlin (1999), Evidence for a wind-driven intensification of the Kuroshio Current Extension from the 1970s to the 1980s, *J. Clim.*, *12*(6), 1697–1706.

Dima, M., and G. Lohmann (2010), Evidence for two distinct modes of large-scale ocean circulation changes over the last century, *J. Clim.*, *23*(1), 5–16.

Easterling, D. R., and M. F. Wehner (2009), Is the climate warming or cooling?, *Geophys. Res. Lett.*, *36*, L08706, doi:10.1029/2009GL037810.

Feldstein, S. B., and C. Franzke (2006), Are the North Atlantic Oscillation and the northern annular mode distinguishable?, *J. Atmos. Sci.*, *63*(11), 2915–2930.

Fu, Q., and P. Lin (2011), Poleward shift of subtropical jets inferred from satellite-observed lower-stratospheric temperatures, *J. Clim.*, *24*(21), 5597–5603.

Fyfe, J. C., and O. A. Saenko (2006), Simulated changes in the extratropical Southern Hemisphere winds and currents, *Geophys. Res. Lett.*, *33*, L06701, doi:10.1029/2005GL025332.

Fyfe, J. C., G. Boer, and G. Flato (1999), The Arctic and Antarctic Oscillations and their projected changes under global warming, *Geophys. Res. Lett.*, *26*(11), 1601–1604.

Giese, B. S., and S. Ray (2011), El Niño variability in simple ocean data assimilation (SODA), 1871–2008, *J. Geophys. Res.*, *116*, C02024, doi:10.1029/2010JC006695.

Gillett, N. P., and J. Fyfe (2013), Annular mode changes in the CMIP5 simulations, *Geophys. Res. Lett.*, *40*, 1189–1193, doi:10.1002/grl.50249.

Gillett, N. P., and D. W. Thompson (2003), Simulation of recent Southern Hemisphere climate change, *Science*, *302*(5643), 273–275.

Goni, G. J., F. Bringas, and P. N. DiNezio (2011), Observed low frequency variability of the Brazil Current front, *J. Geophys. Res.*, *116*, C10037, doi:10.1029/2011JC007198.

Gulev, S., T. Jung, and E. Ruprecht (2007), Estimation of the impact of sampling errors in the VOS observations on air-sea fluxes. Part I: Uncertainties in climate means, *J. Clim.*, *20*(2), 279–301.

Hall, A., and M. Visbeck (2002), Synchronous Variability in the Southern Hemisphere Atmosphere, Sea Ice, and Ocean Resulting from the Annular Mode, *J. Clim.*, *15*(21), 3043–3057.

Hu, Y., and Q. Fu (2007), Observed poleward expansion of the Hadley circulation since 1979, *Atmos. Chem. Phys.*, *7*(19), 5229–5236.

Inatsu, M., H. Mukougawa, and S. Xie (2002), Tropical and extratropical SST effects on the midlatitude storm track, *J. Meteorol. Soc. Jpn.*, *80*(4B), 1069–1076.

Johanson, C. M., and Q. Fu (2009), Hadley cell widening: Model simulations versus observations, *J. Clim.*, *22*(10), 2713–2725.

Kalnay, E., et al. (1996), The NCEP/NCAR 40-year reanalysis project, *Bull. Am. Meteorol. Soc.*, *77*(3), 437–471.

Kelly, K. A., M. J. Caruso, S. Singh, and B. Qiu (1996), Observations of atmosphere-ocean coupling in midlatitude western boundary currents, *J. Geophys. Res.*, *101*(C3), 6295–6312.

Kindem, I. T., and B. Christiansen (2001), Tropospheric response to stratospheric ozone loss, *Geophys. Res. Lett.*, *28*(8), 1547–1550.

Köhl, A. (2015), Evaluation of the GECCO2 ocean synthesis: Transports of volume, heat and freshwater in the Atlantic, *Q. J. R. Meteorol. Soc.*, *141*(686), 166–181.

Köhl, A., and D. Stammer (2008), Variability of the meridional overturning in the North Atlantic from the 50-year GECCO state estimation, *J. Phys. Oceanogr.*, *38*(9), 1913–1930.

Krueger, O., F. Schenk, F. Feser, and R. Weisse (2013), Inconsistencies between long-term trends in storminess derived from the 20cr reanalysis and observations, *J. Clim.*, *26*(3), 868–874.

Kushner, P. J., I. M. Held, and T. L. Delworth (2001), Southern Hemisphere atmospheric circulation response to global warming, *J. Clim.*, *14*(10), 2238–2249.

L'Ecuyer, T. S., and G. L. Stephens (2003), The tropical oceanic energy budget from the TRMM perspective. Part I: Algorithm and uncertainties, *J. Clim.*, *16*(12), 1967–1985.

Lohmann, G., H. Haak, and J. H. Jungclaus (2008), Estimating trends of Atlantic meridional overturning circulation from long-term hydrographic data and model simulations, *Ocean Dyn.*, *58*(2), 127–138.

Lu, J., G. A. Vecchi, and T. Reichler (2007), Expansion of the Hadley cell under global warming, *Geophys. Res. Lett.*, *34*, L06805, doi:10.1029/2006GL028443.

Mantua, N. J., S. R. Hare, Y. Zhang, J. M. Wallace, and R. C. Francis (1997), A Pacific interdecadal climate oscillation with impacts on salmon production, *Bull. Am. Meteorol. Soc.*, *78*(6), 1069–1079.

Marshall, G. J. (2003), Trends in the Southern Annular Mode from observations and reanalyses, *J. Clim.*, *16*(24), 4134–4143.

Meehl, G. A., C. Covey, K. E. Taylor, T. Delworth, R. J. Stouffer, M. Latif, B. McAvaney, and J. F. Mitchell (2007), The WCRP CMIP3 multimodel dataset: A new era in climate change research, *Bull. Am. Meteorol. Soc.*, *88*(9), 1383–1394.

Minobe, S., A. Kuwano-Yoshida, N. Komori, S. P. Xie, and R. J. Small (2008), Influence of the Gulf Stream on the troposphere, *Nature*, *452*(7184), 206–209.

Morice, C. P., J. J. Kennedy, N. A. Rayner, and P. D. Jones (2012), Quantifying uncertainties in global and regional temperature change using an ensemble of observational estimates: The HadCRUT4 data set, *J. Geophys. Res.*, *117*, D08101, doi:10.1029/2011JD017187.

Pedlosky, J. (1996), *Ocean Circulation Theory*, Springer.

Poli, P., et al. (2016), ERA-20C: An atmospheric reanalysis of the 20th century, *J. Clim.*, *29*(11), 4083–4097.

Polvani, L. M., D. W. Waugh, G. J. Correa, and S.-W. Son (2011), Stratospheric ozone depletion: The main driver of twentieth-century atmospheric circulation changes in the southern hemisphere, *J. Clim.*, *24*(3), 795–812.

Previdi, M., and B. G. Liepert (2007), Annular modes and Hadley cell expansion under global warming, *Geophys. Res. Lett.*, *34*, L22701, doi:10.1029/2007GL031243.

Qiu, B. (2003), Kuroshio Extension variability and forcing of the Pacific decadal oscillations: Responses and potential feedback, *J. Phys. Oceanogr.*, *33*(12), 2465–2482.

Qiu, B., and S. Chen (2005), Variability of the Kuroshio Extension jet, recirculation gyre, and mesoscale eddies on decadal time scales, *J. Phys. Oceanogr.*, *35*(11), 2090–2103.

Qiu, B., and S. Chen (2006), Decadal variability in the large-scale sea surface height field of the South Pacific Ocean: Observations and causes, *J. Phys. Oceanogr.*, *36*(9), 1751–1762.

Rahmstorf, S., G. Feulner, M. E. Mann, A. Robinson, S. Rutherford, and E. J. Schaffernicht (2015), Exceptional twentieth-century slowdown in Atlantic Ocean overturning circulation, *Nat. Clim. Change*, *5*(5), 475–480.

Rauthe, M., A. Hense, and H. Paeth (2004), A model intercomparison study of climate change-signals in extratropical circulation, *Int. J. Climatol.*, *24*(5), 643–662.

Rayner, N., D. Parker, E. Horton, C. Folland, L. Alexander, D. Rowell, E. Kent, and A. Kaplan (2003), Global analyses of sea surface temperature, sea ice, and night marine air temperature since the late nineteenth century, *J. Geophys. Res.*, *108*(D14), 4407, doi:10.1029/2002JD002670.

Refsgaard, J. C., et al. (2014), A framework for testing the ability of models to project climate change and its impacts, *Clim. Change*, *122*(1-2), 271–282.

Reynolds, R. W., N. A. Rayner, T. M. Smith, D. C. Stokes, and W. Wang (2002), An improved in situ and satellite SST analysis for climate, *J. Clim.*, *15*(13), 1609–1625.

Ridgway, K. R. (2007), Long-term trend and decadal variability of the southward penetration of the East Australian Current, *Geophys. Res. Lett.*, *34*, L13613, doi:10.1029/2007GL030393.

Ridgway, K., R. Coleman, R. Bailey, and P. Sutton (2008), Decadal variability of East Australian Current transport inferred from repeated high-density XBT transects, a CTD survey and satellite altimetry, *J. Geophys. Res.*, *113*, C08039, doi:10.1029/2007JC004664.

Roemmich, D., J. Gilson, R. Davis, P. Sutton, S. Wijffels, and S. Riser (2007), Decadal spin-up of the South Pacific subtropical gyre, *J. Phys. Oceanogr.*, *37*(2), 162–173.

Rogers, J., and M. McHugh (2002), On the separability of the North Atlantic Oscillation and Arctic Oscillation, *Clim. Dyn.*, *19*(7), 599–608.

Rossow, W. B., and R. A. Schiffer (1991), ISCCP cloud data products, *Bull. Am. Meteorol. Soc.*, *72*(1), 2–20.

Sakamoto, T. T., H. Hasumi, M. Ishii, S. Emori, T. Suzuki, T. Nishimura, and A. Sumi (2005), Responses of the Kuroshio and the Kuroshio Extension to global warming in a high-resolution climate model, *Geophys. Res. Lett.*, *32*, L14617, doi:10.1029/2005GL023384.

Santer, B. D., et al. (2003), Contributions of anthropogenic and natural forcing to recent tropopause height changes, *Science*, *301*(5632), 479–483.

Sasaki, Y. N., and N. Schneider (2011), Decadal Shifts of the Kuroshio Extension Jet: Application of Thin-Jet Theory, *J. Phys. Oceanogr.*, *41*(5), 979–993.

Sato, Y., S. Yukimoto, H. Tsujino, H. Ishizaki, and A. Noda (2006), Response of North Pacific ocean circulation in a Kuroshio-resolving ocean model to an Arctic Oscillation (AO)-like change in Northern Hemisphere atmospheric circulation due to greenhouse-gas forcing, *J. Meteorol. Soc. Jpn.*, *84*(2), 295–309.

Schlesinger, M. E., and N. Ramankutty (1994), An oscillation in the global climate system of period 65-70 years, *Nature*, *367*(6465), 723–726.

Seager, R., Y. Kushnir, N. H. Naik, M. A. Cane, and J. Miller (2001), Wind-Driven Shifts in the Latitude of the Kuroshio-Oyashio Extension and Generation of SST Anomalies on Decadal Timescales, *J. Clim.*, *14*(22), 4249–4265.

Seager, R., D. S. Battisti, J. Yin, N. Gordon, N. Naik, A. C. Clement, and M. A. Cane (2002), Is the Gulf Stream responsible for Europe's mild winters?, *Q. J. R. Meteorol. Soc.*, *128*(586), 2563–2586.

Seidel, D. J., and W. J. Randel (2007), Recent widening of the tropical belt: Evidence from tropopause observations, *J. Geophys. Res.*, *112*, D20113, doi:10.1029/2007JD008861.

Seidel, D. J., Q. Fu, W. J. Randel, and T. J. Reichler (2007), Widening of the tropical belt in a changing climate, *Nat. Geosci.*, *1*(1), 21–24.

Sen Gupta, A., and M. H. England (2006), Coupled ocean-atmosphere-ice response to variations in the Southern Annular Mode, *J. Clim.*, *19*(18), 4457–4486.

Sen Gupta, A., A. Santoso, A. S. Taschetto, C. C. Ummenhofer, J. Trevena, and M. H. England (2009), Projected changes to the Southern Hemisphere ocean and sea ice in the IPCC AR4 climate models, *J. Clim.*, *22*(11), 3047–3078.

Sexton, D. (2001), The effect of stratospheric ozone depletion on the phase of the Antarctic Oscillation, *Geophys. Res. Lett.*, *28*(19), 3697–3700.

Shaman, J., R. Samelson, and E. Skyllingstad (2010), Air-sea fluxes over the Gulf Stream region: Atmospheric controls and trends, *J. Clim.*, *23*(10), 2651–2670.

Stocker, T. F., et al. (2013), Climate Change 2013: The Physical Science Basis. Contribution of Working Group I to the Fifth Assessment Report of the Intergovernmental Panel on Climate Change, edited by T. F. Stocker, et al., 33–115, Cambridge University Press.

Stone, D., A. J. Weaver, and R. J. Stouffer (2001), Projection of climate change onto modes of atmospheric variability, *J. Clim.*, *14*(17), 3551–3565.

Taguchi, B., S.-P. Xie, N. Schneider, M. Nonaka, H. Sasaki, and Y. Sasai (2007), Decadal variability of the Kuroshio Extension: Observations and an eddy-resolving model hindcast, *J. Clim.*, *20*(11), 2357–2377.

Taguchi, B., H. Nakamura, M. Nonaka, and S. Xie (2009), Influences of the Kuroshio/Oyashio Extensions on air-sea heat exchanges and storm-track activity as revealed in regional atmospheric model simulations for the 2003/04 cold season, *J. Clim.*, *22*(24), 6536–6560.

Tang, X., F. Wang, Y. Chen, and M. Li (2009), Warming trend in northern East China Sea in recent four decades, *Chinese J. Oceanol. Limnol.*, *27*, 185–191.

Taylor, K. E., V. Balaji, S. Hankin, M. Juckes, B. Lawrence, and S. Pascoe (2010), CMIP5 Data Reference SyntaxF (DRS) and Controlled Vocabularies.

Taylor, K. E., R. J. Stouffer, and G. A. Meehl (2012), An overview of CMIP5 and the experiment design, *Bull. Am. Meteorol. Soc.*, *93*(4), 485–498.

Thompson, D. W., and S. Solomon (2002), Interpretation of recent Southern Hemisphere climate change, *Science*, *296*(5569), 895–899.

Thompson, D. W., and J. M. Wallace (2000), Annular modes in the extratropical circulation. Part I: Month-to-month variability, *J. Clim.*, *13*(5), 1000–1016.

Thompson, D. W., S. Solomon, P. J. Kushner, M. H. England, K. M. Grise, and D. J. Karoly (2011), Signatures of the Antarctic ozone hole in southern hemisphere surface climate change, *Nat. Geosci.*, *4*(11), 741–749.

Uppala, S. M., et al. (2005), The ERA-40 re-analysis, *Q. J. R. Meteorol. Soc.*, *131*(612), 2961–3012.

Van de Poll, H., H. Grubb, and I. Astin (2006), Sampling uncertainty properties of cloud fraction estimates from random transect observations, *J. Geophys. Res.*, *111*, D22218, doi:10.1029/2006JD007189.

Wang, L., and W. Chen (2010), Downward Arctic Oscillation signal associated with moderate weak stratospheric polar vortex and the cold December 2009, *Geophys. Res. Lett.*, *37*, L09707, doi:10.1029/2010GL042659.

Wu, L., et al. (2012), Enhanced warming over the global subtropical western boundary currents, *Nat. Clim. Change*, *2*(3), 161–166.

Yang, H., J. Liu, G. Lohmann, X. Shi, Y. Hu, and X. Chen (2016), Ocean-atmosphere dynamics changes associated with prominent ocean surface turbulent heat fluxes trends during 1958–2013, *Ocean Dyn.*, *66*(3), 353–365.

Yu, L., X. Jin, and R. A. Weller (2008), Multidecade Global Flux Datasets from the Objectively analyzed Air-sea Fluxes (OAFlux) Project: Latent and Sensible Heat Fluxes, Ocean Evaporation, and Related Surface Meteorological Variables, *OAFlux Project Tech. Rep. OA-2008-01*, 64 pp., Woods Hole, Mass.